

# Metric Engineering of Crystalline Inclusion Compounds by Structural Mimicry\*\*

K. Travis Holman and Michael D. Ward\*

Considerable effort has been devoted to crystal engineering—the skillful contrivance of crystal architecture—of host frameworks capable of guest inclusion.<sup>[1]</sup> The molecular-scale cavities of inclusion hosts can potentially serve as miniaturized reaction chambers,<sup>[2]</sup> catalytic environments,<sup>[3]</sup> and storage compartments<sup>[4]</sup> in a manner that resembles<sup>[5]</sup> more well established zeolites. Though interpenetration<sup>[6]</sup> and the unpredictability of molecular assembly complicate the design of low-density host frameworks, strategies that rely on modular design<sup>[7]</sup>—using robust supramolecular building blocks—promise improved control of solid-state structure. However, modular strategies also require elucidation of the intermolecular forces and molecular recognition factors that govern host–guest organization, so that crystal architecture and specific metric parameters can be reliably predicted and ultimately controlled. We herein report a rare example of crystal engineering in which the host–guest organization and specific structural features of a series of new inclusion compounds can be anticipated from the known crystal structures of the pure guests.

Recent efforts in our laboratory have produced a family of lamellar inclusion compounds based upon a persistent two-dimensional quasihexagonal hydrogen-bonding sheet comprising guanidinium cations (G) and the sulfonate (S) moieties of organodisulfonate anions,<sup>[8]</sup> the latter serving as “pillars” that connect opposing GS sheets to create porous galleries, occupied by guest molecules, between the sheets (Figure 1). The use of different pillars—for example, 1,4-butanedisulfonate, 1,5-naphthalenedisulfonate, 2,6-naphthalenedisulfonate (NDS), 4,4'-biphenyldisulfonate (BPDS), azobenzene-4,4'-disulfonate, or 2,6-anthracenedisulfonate (ADS; Scheme 1)<sup>[9]</sup>—permits adjustment of pore size and character.<sup>[10]</sup> Two compositionally equivalent architectural isomers, a discrete bilayer and a continuous “brick”, can be generated, with the more open, lower density brick architecture templated by larger guest molecules.<sup>[10c, 11]</sup>

The GS inclusion frameworks possess an intrinsic “softness” associated with conformational and turnstilelike rotational freedom of the pillars, as well as accordionlike puckering of the GS sheets about an axis defined by hydrogen bonds that join 1D N–H···O hydrogen-bonded ribbons. These features enable the GS host framework to “shrink-wrap” about a variety of differently sized guest molecules so

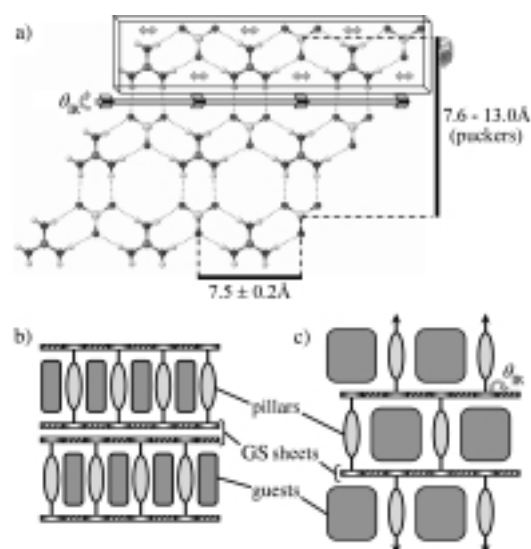
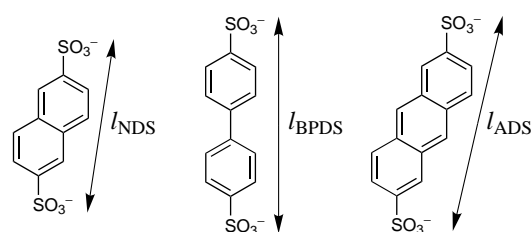


Figure 1. a) The quasihexagonal 2D hydrogen-bonded GS sheet consisting of connected 1D ribbons (boxed) that can pucker by angle  $\theta_{IR}$ . b) Pillared discrete bilayer. c) Pillared continuous “brick” architecture.



Scheme 1. Pillars of 2,6-naphthalenedisulfonate (NDS), 4,4'-biphenyldisulfonate (BPDS), and 2,6-anthracenedisulfonate (ADS) with the corresponding S–S distances  $l$  (8.5, 10.6, and 10.8 Å for NDS, BPDS, and ADS, respectively).

that dense packing, which provides the cohesive energy required for crystallization, can be achieved.

The range of repeat distances within each GS ribbon for the GS host frameworks and their related guanidinium organomonosulfonates is rather narrow ( $7.5 \pm 0.2$  Å), reflecting the stiffness of these ribbons. However, the repeat distance normal to the ribbon direction varies with the interribbon puckering angle ( $\theta_{IR}$ ),<sup>[12]</sup> and ranges from 7.6 Å for highly puckered sheets (e.g.  $\theta_{IR} = 81^\circ$  for  $G_2$ (BPDS)·1,4-dibromobenzene)<sup>[10c]</sup> to 13.0 Å for perfectly flat sheets (e.g.  $\theta_{IR} = 180^\circ$  for  $[G][\text{triflate}]$ ).<sup>[8a]</sup> Interestingly, the dimensions of the 2D herringbone motifs observed in some crystalline aromatic hydrocarbons—such as naphthalene, biphenyl, and anthracene (Figure 2a–c)<sup>[13]</sup>—are within the range of lattice parameters that can be achieved by the flexible GS sheet. This prompted us to examine GS inclusion compounds in which the organic portion of the pillar and the guest were identical so that pillar–guest ensembles, mimicking the herringbone motif of the crystalline guests alone, would form within the galleries. Simple steric and geometric considerations dictate that such a herringbone motif is not sterically possible in the bilayer GS framework. Consequently, this structural mimicry would require the host framework to adopt the more open brick architecture (Figure 2d).

[\*] Prof. Dr. M. D. Ward, Dr. K. T. Holman  
Department of Chemical Engineering and Materials Science  
University of Minnesota  
Minneapolis, MN 55455 (USA)  
Fax: (+1) 612-626-7246  
E-mail: wardx004@tc.umn.edu

[\*\*] This work was supported in part by the MRSEC Program of the National Science Foundation (Award Number DMR-9809364) and by the Natural Sciences and Engineering Research Council of Canada (postdoctoral fellowship for K.T.H.).

Supporting information for this article is available on the WWW under <http://www.wiley-vch.de/home/angewandte/> or from the author.

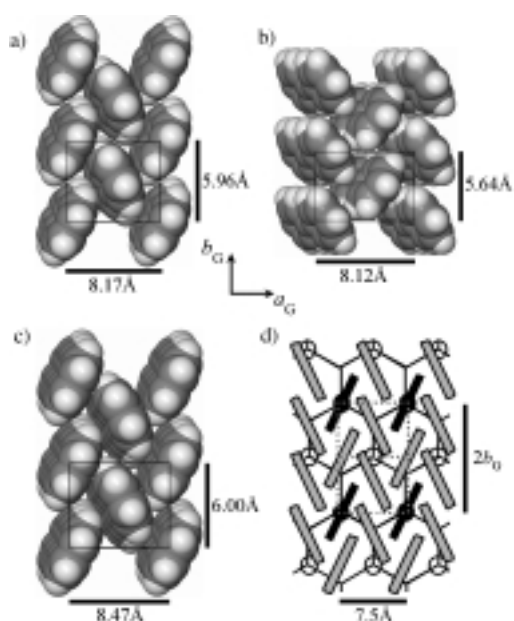


Figure 2. The 2D herringbone motif in a) naphthalene, b) biphenyl, and c) anthracene as viewed normal to the  $ab$  plane. d) Anticipated herringbone pillar-guest packing in the brick framework, as viewed normal to a GS sheet, with a 1:3 stoichiometry of pillar (black) to guest (gray). The pillars projecting below the sheet are depicted as open circles. The correspondence between the GS structure and that of the pure guest crystals is depicted by the dashed rectangles, which represent two unit cells of the herringbone-packed guests.

Compounds  $G_2(\text{NDS}) \cdot 3$  naphthalene (**1**),  $G_2(\text{BPDS}) \cdot 3$  biphenyl (**2**), and  $G_2(\text{ADS}) \cdot 3$  anthracene (**3**) precipitate as single crystals when saturated methanolic solutions of the host components are treated with saturated solutions of the guests. The composition of each compound was confirmed by  $^1\text{H}$  NMR spectroscopy, thermogravimetric analysis (TGA),<sup>[14]</sup> and single-crystal X-ray diffraction.<sup>[15]</sup> These compounds are essentially isostructural, the host frameworks adopting the continuous brick architecture with the guests and their isostructural pillars packing between the GS sheets in a manner nearly identical to that observed in the crystal

structures of the respective pure guests (Figure 3a). As expected, the organodisulfonate pillars effectively replace every fourth molecule in the herringbone motif of the pure guests to afford a pillar:guest stoichiometry of 1:3.

The herringbone pillar-guest ensembles in **1–3** can be described by the in-plane lattice dimensions of the pillar-guest ensembles, defined by two lattice constants:  $b_1$ , coinciding with the relatively stiff GS ribbons, and  $b_2$ , the repeat distance normal to the ribbons, which through puckering can conform to optimize the pillar-guest packing so that  $b_2 \approx 2b_G$ , where  $b_G$  is the  $b$  axis of the pure guest structure ( $b_1 = a$  and  $b_2 = c$  for **1** and **2**;  $b_1 = a$  and  $b_2 = b$  for **3**). The herringbone motif can also be described by the average dihedral angles  $\phi$  between the mean planes of the arenes. Though the stiffness of the GS ribbons along the ribbon direction prevents  $b_1$  from conforming exactly with  $a_G$  of the corresponding pure guests, the  $7.5 \pm 0.2$  Å repeat distance along the GS ribbon is within 8% of  $a_G$ , with **3** having the largest mismatch. However, the values of  $b_2$ , the variable puckering lattice parameter, are nearly identical to  $2b_G$  of the respective guests (Table 1). The pillar-guest ensemble in each inclusion compound exhibits more than one value of  $\phi$ , but the average of these values is nearly identical to the arene-arene dihedral angle in the respective pure guests.<sup>[16]</sup> This reflects the ability of the pillars to rotate about their long axes, which is crucial to achieving the herringbone motif.

All the unit cell angles in **1–3** are equal to, or very near,  $90^\circ$ . The angle subtended by  $b_1$  and  $b_2$  in **1** and **2** ( $\beta$  in the monoclinic cell) deviates slightly from  $90^\circ$  ( $\beta = 91.61^\circ$  and  $90.46^\circ$ , respectively) because of a small misregistry, along the ribbon direction, between adjacent hydrogen-bonded ribbons. In contrast, the angle subtended by  $b_1$  and  $b_2$  in **3** ( $\gamma$  for this compound) is exactly  $90^\circ$ . We note that the brick framework enforces a near-orthorhombic structure in which the long axes of the pillars are normal, or nearly so, to the GS sheets.

The value of  $\theta_{\text{IR}}$ , reflecting the degree of host puckering required to achieve the value of  $b_2$  necessary for herringbone packing, can be predicted by Equation (1), which only requires  $b_G$  (the 6.5 Å term in the denominator corresponds

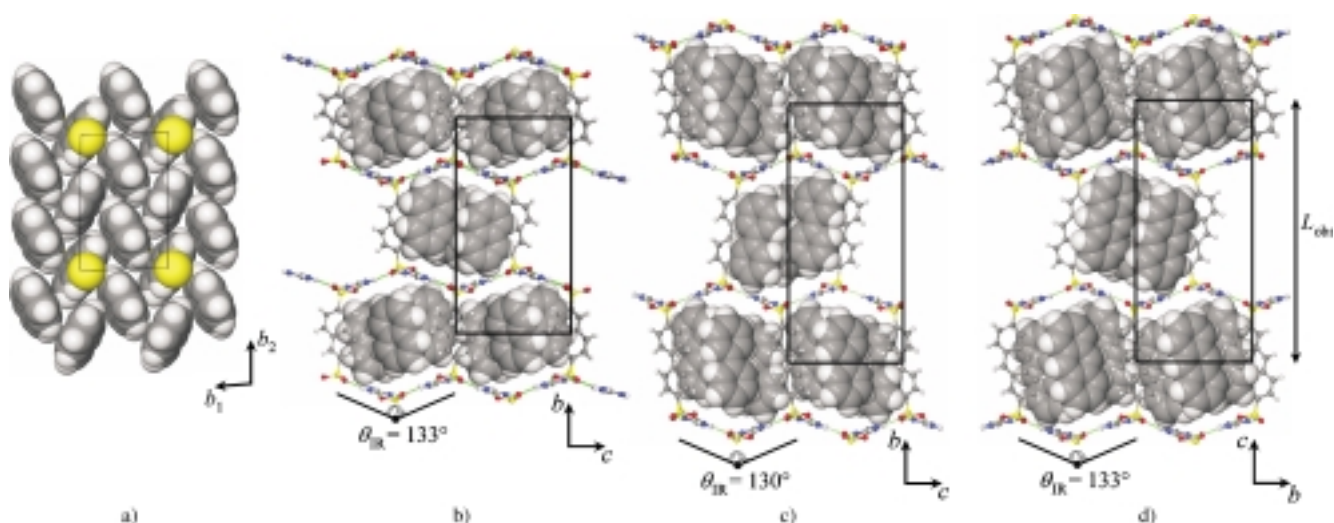


Figure 3. a) Herringbone pillar-guest packing in the  $ab$  plane of **1**. The G ions and sulfonate oxygen atoms have been removed for clarity. Sulfur atoms are yellow. b)–d) The crystal structures of **1**, **2**, and **3** as viewed along the  $a$  axis. The observed interribbon puckering angles  $\theta_{\text{IR}}$  are provided below each structure.

Table 1. Comparison of the structural parameters of GS inclusion compounds and pure guest structures.

Compound	$b_{1,\text{obs}}$ and $a_{\text{G}}$ [Å]	$b_{2,\text{obs}}$ and $2b_{\text{G}}$ [Å]	$\theta_{\text{IR,obs}}$ [°]	$\theta_{\text{IR,calcd}}$ [°]	$L_{\text{obs}}$ [Å]	$L_{\text{calcd}}$ [Å]	$\phi$ [°]
<b>1</b>	$b_1 = 7.64$	$b_2 = 11.82$	133	133	22.04	22.2	54
naphthalene	$a_{\text{N}} = 8.17$	$2b_{\text{N}} = 11.92$					52
<b>2</b>	$b_1 = 7.66$	$b_2 = 11.49$	130	120	26.31	27.7	62
biphenyl	$a_{\text{B}} = 8.12$	$2b_{\text{B}} = 11.28$					67
<b>3</b>	$b_1 = 7.56$	$b_2 = 11.96$	133	135	26.85	26.6	51
anthracene	$a_{\text{A}} = 8.47$	$2b_{\text{A}} = 12.00$					51

$$\theta_{\text{IR,calcd}} = 2 \sin^{-1}(b_{\text{G}}/6.5 \text{ Å}) \quad (1)$$

to one-half of the in-plane 13.0 Å repeat distance normal to the ribbons in a flat GS sheet). With the  $b_{\text{G}}$  lattice parameters of the pure naphthalene, biphenyl, and anthracene guests, Equation (1) affords  $\theta_{\text{IR,calcd}}$  values of 133°, 120°, and 135°, which compare favorably to  $\theta_{\text{IR,obs}}$  values measured from the crystal structures of **1–3** (Table 1).

The lattice constant normal to the GS sheets ( $L$ , given in Å), which defines two lamellae, can be calculated with Equation (2), using  $\theta_{\text{IR,calcd}}$  and  $l$ , the S–S distance of the organodisulfonate pillar measured from known compounds (see Scheme 1). The bilamellar spacings for **1–3**, calculated with Equation (2), agree to within 1 % of the observed values ( $L_{\text{obs}}$ ) for **1** and **3**, and to within 6 % for **2** (Table 1).

$$L_{\text{calcd}} = 2b_{\text{G}}/\tan(\theta_{\text{IR,calcd}}/2) + 2l \quad (2)$$

The agreement of  $b_2$  and  $\phi$  with the corresponding values in the pure guest structure, and of  $\theta_{\text{IR,obs}}$  and  $L_{\text{obs}}$  with calculated values based on the pure guest lattice constant  $b_{\text{G}}$ , strongly argues that the major driving force for pillar–guest organization in the inclusion compounds is the achievement of an innate herringbone motif that mimics molecular organization in the pure guests. The intermolecular forces amongst the guest molecules and their isostructural pillars are sufficient to cause puckering, to a predictable extent, of the soft hydrogen-bonded GS sheets so that the herringbone motif is achieved.

Recently, it was suggested that a 2D pyrene guest network, interpenetrated with a 2D transition metal coordination network, exhibited edge-to-face interactions between the pyrene molecules in a manner reminiscent of molecular packing in many aromatic compounds.<sup>[17]</sup> The brick inclusion compounds described here, as well others reported previously by our laboratory,<sup>[10c]</sup> also can be described as interpenetrated 2D networks. However, compounds **1–3** are distinct—the existence of isostructural framework components, in this case freely rotating pillars, allows the ensemble of pillars and guests to mimic, almost exactly, the molecular packing in the crystal structures of the guests alone.

The ability to tune the guest environment in inclusion cavities of the GS frameworks suggests that crystallization-based separations can be developed in which guest inclusion selectivity is governed by carefully designed host frameworks that permit molecular organization mimicking innate packing motifs, such as the herringbone structures described above. We note the extremely low density of the host frameworks in these clathrates. Indeed, the packing fractions of **1**, **2**, and **3** in the absence of the guests (framework only) are 0.31, 0.29, and

0.29, respectively.<sup>[18]</sup> The guests, in fact, occupy more volume than the host frameworks, with packing fractions of 0.38, 0.39, and 0.43. The corresponding guest mass fractions are 48.6, 51.7, and 54.0 %, illustrating that high separation efficiencies are feasible with protocols based on these inclusion frameworks.

Received: December 9, 1999 [Z14380]

- [1] a) E. Weber, *Top. Curr. Chem.* **1987**, *140*, 1–20, and references therein; b) *Comprehensive Supramolecular Chemistry*, Vol. 6 (Eds.: J. L. Atwood, J. E. D. Davies, D. D. MacNicol, F. Vögtle, K. S. Suslick), Pergamon, Oxford, **1996**.
- [2] a) M. Miyata in *Comprehensive Supramolecular Chemistry*, Vol. 10 (Eds.: J. L. Atwood, J. E. D. Davies, D. D. MacNicol, F. Vögtle, K. S. Suslick), Pergamon, Oxford, **1996**, pp. 557–582; b) Y.-H. Kiang, G. B. Gardner, S. Lee, Z. Xu, E. B. Lobkovsky, *J. Am. Chem. Soc.* **1999**, *121*, 8204–8215.
- [3] Y. Aoyama, K. Endo, T. Anzai, Y. Yamaguchi, T. Sawaki, K. Kobayashi, N. Kanehisa, H. Hashimoto, Y. Kai, H. Masuda, *J. Am. Chem. Soc.* **1996**, *118*, 5562–5571.
- [4] a) D. D. MacNicol, S. J. Rowan in *Comprehensive Supramolecular Chemistry*, Vol. 10 (Eds.: J. L. Atwood, J. E. D. Davies, D. D. MacNicol, F. Vögtle, K. S. Suslick), Pergamon, Oxford, **1996**, pp. 417–428; b) F. Toda, S. Hyoda, K. Okada, K. Hirotsu, *J. Chem. Soc. Chem. Commun.* **1995**, 1531–1532.
- [5] a) S. S.-Y. Chui, S. M.-F. Lo, J. P. H. Charmant, A. G. Orpen, I. D. Williams, *Science*, **1999**, *283*, 1148–1150; b) L. Hailian, A. Laine, M. O'Keefe, O. M. Yaghi, *Science* **1999**, *283*, 1145–1147; c) M. Kondo, T. Okubu, A. Asami, S. Noro, T. Yoshitomi, S. Kitagawa, T. Ishii, H. Matsuzaka, K. Seki, *Angew. Chem.* **1999**, *111*, 190–193; *Angew. Chem. Int. Ed.* **1999**, *38*, 140–143; d) P. Brunet, M. Simard, J. D. Wuest, *J. Am. Chem. Soc.* **1997**, *119*, 2737–2738.
- [6] S. R. Batten, R. Robson, *Angew. Chem.* **1998**, *110*, 1558–1595; *Angew. Chem. Int. Ed.* **1998**, *37*, 1460–1494, and references therein.
- [7] a) *Proceedings of the NATO Advanced Research Workshop on Modular Chemistry* (Ed.: J. Michl), Kluwer, Boston, **1997**; b) G. R. Desiraju, *Angew. Chem.* **1995**, *107*, 2541–2558; *Angew. Chem. Int. Ed. Engl.* **1995**, *34*, 2311–2327; c) M. D. Ward, *Pure Appl. Chem.* **1992**, *64*, 1623–1627.
- [8] a) V. A. Russell, M. C. Etter, M. D. Ward, *J. Am. Chem. Soc.* **1994**, *116*, 1941–1952; b) V. A. Russell, M. C. Etter, M. D. Ward, *Chem. Mater.* **1994**, *6*, 1206–1217; c) V. A. Russell, M. D. Ward, *J. Mater. Chem.* **1997**, *7*, 1123–1133.
- [9] M. F. Acquavella, M. E. Evans, S. W. Farraher, C. J. Névoret, C. J. Abelt, *J. Org. Chem.* **1994**, *59*, 2894–2897.
- [10] a) V. A. Russell, C. C. Evans, W. Li, M. D. Ward, *Science* **1996**, *276*, 575–579; b) J. A. Swift, A. M. Reynolds, M. D. Ward, *Chem. Mater.* **1998**, *10*, 4159–4168; c) J. A. Swift, A. M. Pivovar, A. M. Reynolds, M. D. Ward, *J. Am. Chem. Soc.* **1998**, *120*, 5887–5894; d) C. C. Evans, L. Sukarto, M. D. Ward, *J. Am. Chem. Soc.* **1998**, *121*, 320–325.
- [11] Numerous examples of  $G_2(\text{BPDS}) \cdot n\text{guest}$  inclusion compounds suggest a critical guest volume for the bilayer-to-brick conversion of about 128 Å<sup>3</sup>.
- [12] The value of  $\theta_{\text{IR}}$  was determined from the angle subtended by the centroid of two sulfur atoms on a selected GS ribbon and the nearest sulfur atom on the two adjacent ribbons.

- [13] a) Naphthalene: C. P. Brock, J. D. Dunitz, *Acta Cryst. Sect. B* **1982**, *38*, 2218–2228; b) biphenyl: J. Trotter, *Acta Cryst.* **1961**, *14*, 1135–1139; c) anthracene: C. P. Brock, J. D. Dunitz, *Acta Cryst. Sect. B* **1990**, *46*, 795–806.
- [14] Weight percent of guest loss by TGA (obs/calcd): **1**: 48.6/48.6, **2**: 51.8/51.7, **3**: 52.5/54.0.
- [15] A full hemisphere of data was collected on a Siemens SMART diffractometer with Mo $\alpha_K$  radiation ( $\lambda = 0.71073$  Å). Data were corrected for Lorentz polarization, absorption, and decay using SADABS. Structures were solved by direct methods (SHELXS) and refined with full-matrix least squares based on  $|F^2|$  (SHELXL-97-2). Hydrogen atoms were placed in calculated positions using a riding model. X-ray data for **1** (C<sub>21</sub>H<sub>21</sub>N<sub>3</sub>O<sub>3</sub>S): 0.42 × 0.36 × 0.21 mm, monoclinic,  $P2_1/n$  (no. 14),  $a = 7.6376(1)$ ,  $b = 22.0442(4)$ ,  $c = 11.8162(1)$  Å,  $\beta = 91.611(1)^\circ$ ,  $Z = 4$ ,  $V = 1988.65(5)$  Å<sup>3</sup>,  $\rho_{\text{calcd}} = 1.321$  g cm<sup>-3</sup>,  $\mu = 0.190$  mm<sup>-1</sup>,  $1.8 < 2\theta < 24.0^\circ$ ,  $T = 173$  K,  $R_1 = 0.0351$  and  $wR_2 = 0.0819$  for 2621 ( $I > 2\sigma[I]$ ) of 3107 unique reflections and 253 parameters. X-ray data for **2** (C<sub>25</sub>H<sub>25</sub>N<sub>3</sub>O<sub>3</sub>S): 0.49 × 0.22 × 0.22 mm, monoclinic,  $P2_1/n$  (no. 14),  $a = 7.6612(6)$ ,  $b = 26.306(2)$ ,  $c = 11.4887(9)$  Å,  $\beta = 90.458(2)^\circ$ ,  $Z = 4$ ,  $V = 2315.3(3)$  Å<sup>3</sup>,  $\rho_{\text{calcd}} = 1.284$  g cm<sup>-3</sup>,  $\mu = 0.171$  mm<sup>-1</sup>,  $1.5 < 2\theta < 25.0^\circ$ ,  $T = 173$  K,  $R_1 = 0.0359$  and  $wR_2 = 0.0920$  for 3086 ( $I > 2\sigma[I]$ ) of 4084 unique reflections and 289 parameters. X-ray data for **3** (C<sub>29</sub>H<sub>30</sub>N<sub>3</sub>O<sub>3</sub>S): 0.24 × 0.09 × 0.03 mm, monoclinic,  $P2_1/n$  (no. 14),  $a = 7.559(5)$ ,  $b = 11.96(1)$ ,  $c = 26.85(2)$  Å,  $\beta = 94.17(8)^\circ$ ,  $Z = 4$ ,  $V = 2422(3)$  Å<sup>3</sup>,  $\rho_{\text{calcd}} = 1.36$  g cm<sup>-3</sup>,  $\mu = 0.171$  mm<sup>-1</sup>,  $1.9 < 2\theta < 24.0^\circ$ ,  $T = 173$  K,  $R_1 = 0.2791$  and  $wR_2 = 0.5839$  for 2704 ( $I > 2\sigma[I]$ ) of 3801 unique reflections and 186 parameters. The highly mosaic nature of all samples made accurate integration of the reflection intensities difficult and precluded the possibility of a more accurate single-crystal structure determination for compound **3**. We surmise that the high mosaicity can be attributed to the larger lattice mismatch (8%), compared to **1** and **2**, between the host structure and the native anthracene structure. X-ray powder diffraction of the bulk material (see the Supporting Information) reveals a unit cell identical to that determined from the single-crystal data and, based upon extensive studies of closely related compounds, confirms the structural assignment of the brick architecture for **3**. Importantly, the metric parameters with which this manuscript is principally concerned (i.e.,  $b_1$  and  $b_2$ ) can be obtained from the lattice constants. Crystallographic data (excluding structure factors) for the structures reported in this paper have been deposited with the Cambridge Crystallographic Data Centre as supplementary publication nos. CCDC-136727 (**1**), -136728 (**2**), and -136729 (**3**). Copies of the data can be obtained free of charge on application to CCDC, 12 Union Road, Cambridge CB2 1EZ, UK (fax: (+44) 1223-336-033; e-mail: deposit@ccdc.cam.ac.uk).
- [16] Unique interplanar dihedral angles in **1**: 51°, 56°; **2**: 57°, 67°, 56°, 66°; **3**: 47°, 54°. A subtle difference between the inclusion compounds and the pure guest structures is the nonparallelism between face-to-face arenes in **1–3** (**1**: 14°; **2**: 5°; **3**: 10°).
- [17] K. Biradha, K. V. Domasevitch, B. Moulton, C. Seward, M. J. Zaworotko, *Chem. Commun.* **1999**, 1327–1328.
- [18] Packing fraction calculations performed with Molecular Simulations Inc. Cerius<sup>2</sup> (v. 3.5) software using a probe radius of 0.5 Å.

## The Eight Stereoisomers of LNA (Locked Nucleic Acid): A Remarkable Family of Strong RNA Binding Molecules\*\*

Vivek K. Rajwanshi, Anders E. Håkansson, Mads D. Sørensen, Stefan Pitsch, Sanjay K. Singh, Ravindra Kumar, Poul Nielsen, and Jesper Wengel\*

For more than a decade, chemists have searched the chemical space in order to obtain nucleic acid analogues with certain desirable properties, such as increased stability towards nucleolytic degradation and increased binding affinity (and specificity) towards complementary natural nucleic acid targets.<sup>[1]</sup> A strong impetus for this research has been, and continues to be, the therapeutic promises of the antisense strategy.<sup>[2]</sup> Unprecedented thermal affinities of duplexes involving the nucleic acid analogue “LNA” (Locked Nucleic Acid, **T<sup>L</sup>**,  $\beta$ -D-ribo isomer, Figure 1) have recently been reported by us<sup>[3,4]</sup> and others.<sup>[5]</sup> The furanose ring of LNA, being part of a dioxabicyclo[2.2.1]heptane skeleton, is efficiently locked in a C-3'-endo (N-type) conformation and we have initiated a program which focuses on the synthesis and properties of the likewise conformationally locked configurational isomers of LNA. Recently we have published the syntheses of the two first diastereoisomeric forms of LNA, namely “xylo-LNA” (**xT<sup>L</sup>**,  $\beta$ -D-xylo isomer) and “ $\alpha$ -L-LNA” ( **$\alpha$ T<sup>L</sup>**,  $\alpha$ -L-ribo isomer, Figure 1).<sup>[6,7]</sup>

In this report, the RNA binding of all eight possible stereoisomers of LNA is evaluated. Synthesis of “ $\alpha$ -L-xylo-LNA” ( **$\alpha$ xT<sup>L</sup>**,  $\alpha$ -L-xylo isomer,<sup>[7]</sup> Figure 1) has been accomplished and the remaining four stereoisomers (Figure 1), all enantiomers of the four synthesized diastereoisomers, are indirectly evaluated by hybridization studies of the four synthesized stereoisomers towards enantiomeric RNA targets (ent-RNA, also known as L-RNA or mirror-image RNA).<sup>[8]</sup>

In Table 1 the results from hybridization studies towards RNA complements for homo-thymine derivatives are shown. Whereas the remarkable binding affinities of fully modified<sup>[7]</sup> LNA,  $\alpha$ -L-LNA, and xylo-LNA have been reported earlier,<sup>[3,6b]</sup> it can be seen that fully modified  $\alpha$ -L-xylo-LNA [5'-( **$\alpha$ xT<sup>L</sup>**)<sub>9</sub>T] is unable to hybridize towards both RNA and ent-RNA.<sup>[9]</sup> The reason for this is presently unclear but the

[\*] Prof. Dr. J. Wengel, Dr. V. K. Rajwanshi, A. E. Håkansson, M. D. Sørensen, Dr. S. K. Singh, Dr. R. Kumar  
Center for Synthetic Bioorganic Chemistry  
Department of Chemistry, University of Copenhagen  
Universitetsparken 5, 2100 Copenhagen (Denmark)  
Fax: (+45) 35-32-02-12  
E-mail: wengel@kiku.dk

Dr. S. Pitsch  
Laboratorium für Organische Chemie  
ETH-Zentrum, Zürich (Switzerland)

P. Nielsen  
Department of Chemistry  
University of Southern Denmark, Odense (Denmark)

[\*\*] We acknowledge the Danish Natural Science Research Council, the Danish Technical Research Council, and Exiqon A/S for financial support. Ms Britta M. Dahl is thanked for oligonucleotide synthesis, Dr. Carl E. Olsen for MALDI-MS analysis, and Ms. Karen Jørgensen for recording CD spectra.